

A 300 GHz "Always-In-Focus" Focusing System for Target Detection

Javier MONTERO-DE-PAZ, Luis Enrique GARCIA-MUÑOZ, Daniel SEGOVIA-VARGAS

Dept. of Signal Theory and Communications, Carlos III University of Madrid (UC3M),
Avenida de la Universidad 30, 28911, Leganés, Spain

jmontero@tsc.uc3m.es, legarcia@tsc.uc3m.es, dani@tsc.uc3m.es

Abstract. *A focusing system for a 300 GHz radar with 5 m target distance and 10 mm diameter spot size resolution is proposed. The focusing system is based on a Gaussian telescope scheme and its main parameters have been designed using Gaussian beam quasi-optical propagation theory with an in-house developed MATLAB® based analysis tool. Then, this approach has been applied to a real focusing system based on two elliptical mirrors in order to reduce the distortion and cross-polar level and a plane mirror to provide scanning capabilities. The overall system has been simulated with a full-wave electromagnetic simulator and its behavior is presented. With this approach, the focusing system always works "in-focus" since the only mirror that is rotated when scanning is the output plane mirror, so the beam is almost not distorted. The design process, although based in the well-known Gaussian beam quasi-optical propagation theory, provides a fast and accurate method and minimizes the overall size of the mirrors. As a consequence, the size of the focusing system is also reduced.*

Keywords

Quasi-optical Gaussian beam propagation, radar, focusing system, terahertz imaging.

1. Introduction

Terahertz (THz) frequency band or electromagnetic signals at terahertz frequencies (0.1 THz – 10 THz) is receiving great attention in the electromagnetism community nowadays. This band has been traditionally associated with radio-astronomy works and molecular spectroscopy. At these frequencies, extremely short pulses can be generated, which are capable of obtaining high spatial resolutions, go across light opaque materials and visualize and identify microscopic structures by spectral analysis. Moreover, there exists a great interest in different applications of this technology such as defense and security, automobiles, biology and medicine [1].

One of the main applications of this technology is target detection for security purposes. This comes from the fact that most clothes and envelopes are reasonably trans-

parent at these frequencies while, at the same time, high image resolution can be achieved. Nowadays, a great effort is being made in designing terahertz imaging systems for different purposes [2]-[10].

In order to identify objects hidden behind envelopes or clothes, a very high resolution (on the order of mm or cm) is needed and, for most cases, the target is placed at distances larger than a meter away from the radar. With these assumptions, a focusing system with very high directivity (and very high resolution as a consequence) is desirable. Such high directivity can only be obtained by using an array of antennas or a parabolic or elliptical mirror. In both cases, the structure is very big in terms of the wavelength, so a large number of computational resources and relatively long periods of time to carry out appropriate calculations are required. A tool capable of providing fast and accurate approximation of the performance of an electromagnetic system in the range of quasi-optics is desirable and welcome. The goal is not to completely solve the electromagnetic problem, but to develop a technique that greatly reduces the computation time, based on the theory of propagation of Gaussian beams [11]. Once the main variables are obtained, the whole electromagnetic problem can be solved using commercial full-wave electromagnetic antenna software [12].

In this paper a focusing system for a 300 GHz radar with 5 m target distance and 10 mm diameter spot size resolution, defined as the -3 dB beamwidth, is proposed. The objective afterwards is to include this focusing system in a terahertz radar, so the signal generation, as long as the digital signal processing units, must be included thereafter. This will be presented in a separate paper. In addition, a fast and accurate design method which finds the optimal parameters and reduces the overall computation time is presented. The resulting focusing system is formed by two elliptical mirrors to reduce the distortion and cross-polar level [13]-[15] and a planar one to provide scanning capabilities. It has to be mentioned that the only rotating mirror to provide scanning capabilities is the plane one, so this simple scheme reduces the complexity of previous solutions. Its main advantage is that it always works "in-focus", what means that the beam is almost not distorted when scanning the target. The overall system is designed in such a way that the output focus of the second elliptical mirror is

5 m away from it (target detection distance) so when the plane mirror is rotated the output focus is displaced but it is always 5 m away from the second elliptical mirror.

The paper is organized as follows: First, the whole system is proposed and the feeding element is presented. In addition, the focusing system is analyzed using Gaussian beam Quasi-Optical (QO) propagation and the main parameters are obtained. Then those QO parameters are applied to the design of real sized parameters elliptical mirrors to obtain the actual focusing system. This system is validated using full-wave electromagnetic antenna software [12] and the obtained results are presented. Finally, some conclusions and future lines are introduced.

2. System Design

In this section the proposed system is presented and an analysis based on Gaussian beam QO propagation [11] is performed. The design is based on a Gaussian beam telescope, where the separation between the two focusing elements is the sum of their focal lengths. Fig. 1 shows a schematic of the proposed focusing system. In this section they will be represented as thin lenses in order to simplify QO calculations while in Section 3 they will be replaced with elliptical mirrors. Elliptical mirrors have been chosen because, if properly designed, they can reduce the distortion effects and the cross polar level [13]-[15]. Moreover, a paraboloid system (more than one paraboloid) has less degrees of freedom in the design and a relatively high blockage inevitably happens [11].

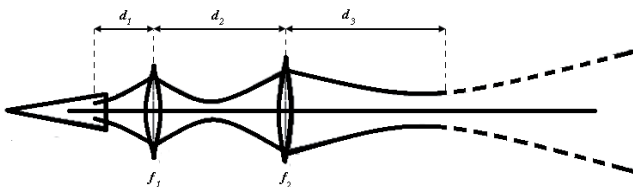


Fig. 1. Quasi-optical path schematic of the Gaussian beam telescope.

2.1 Feeding Element

A corrugated conical horn antenna has been chosen as the feeding source for the system, since it provides a very good Gaussian beam over, at least, 1.5:1 frequency range [11]. Moreover, it can handle more power than any of the current antennas working at these frequencies. Its dimensions are $L_h = 20$ mm and $a = 3.3$ mm (see Fig. 2), which are typical ones for 300 GHz operation ($\lambda = 1$ mm). With these values the beam waist (ω_0) and the location of that beam waist (z_0) can be obtained as [11], [16]:

$$\omega_0^2 = \frac{(0.644 \cdot a)^2}{1 + 0.644^4 \cdot \left(\frac{\pi a^2}{\lambda L_h}\right)^2}, \quad (1)$$

$$z_0 = L_h - \frac{(0.644 \cdot a)^2 \cdot \pi^2 \cdot \omega_0^2}{L_h \cdot \lambda^2}. \quad (2)$$

In our particular case, $\omega_0 = 1.7$ mm and $z_0 = 13.3$ mm, so distance from the beam waist of the horn to its aperture is 6.7 mm ($L_h - z_0 = 20$ mm - 13.3 mm = 6.7 mm). Other QO parameters shown in Fig. 2 are the distance from the beam waist (z), the beam radius at that position (ω) and the radius of curvature at z (R_z). The predicted -3 dB beam-width of the horn is 6.1° while its directivity is 24.1 dBi in the farfield.

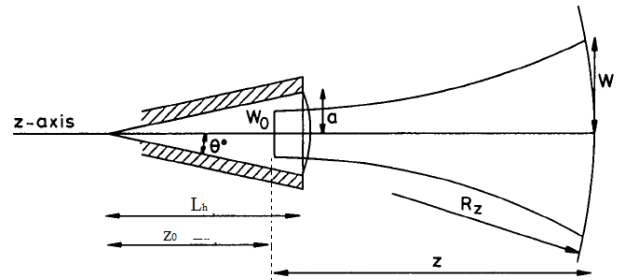


Fig. 2. Corrugated conical horn antenna [16].

2.2 QO Design

Taking advantage of the developed tool [17], [18], it is possible now to quickly calculate the main parameters of our system. The parameters associated to the feed have already been calculated, so it is necessary to calculate the other ones in order to obtain a resolution of 10 mm diameter spot size at 5 m.

Based on the QO Gaussian beam propagation theory the following ABCD matrix for the system shown in Fig. 1 is obtained [11]:

$$\begin{bmatrix} A & B \\ C & D \end{bmatrix} = \begin{bmatrix} 1 & d_3 \\ 0 & 1 \end{bmatrix} \cdot \begin{bmatrix} 1 & 0 \\ -1/f_2 & 1 \end{bmatrix} \cdot \begin{bmatrix} 1 & d_2 \\ 0 & 1 \end{bmatrix} \cdot \begin{bmatrix} 1 & 0 \\ -1/f_1 & 1 \end{bmatrix} \cdot \begin{bmatrix} 1 & d_1 \\ 0 & 1 \end{bmatrix} \quad (3)$$

Distance d_1 has been considered as the distance from the beam waist of the horn antenna to the first thin lens; d_2 is the distance between the two thin lenses; and d_3 the target distance (not the distance from the second thin lens to the output beam waist).

From the ABCD matrix the output beam parameter of the system (q_{out}) can be obtained as [11]:

$$q_{out} = \frac{A \cdot q_{in} + B}{C \cdot q_{in} + D} \quad (3)$$

where q_{in} is the input beam parameter of the system which depends on the feeding element in the following way:

$$q_{in} = \frac{j\pi\omega_0^2}{\lambda} \quad (4)$$

with ω_0 the beam waist of the horn antenna. The beam radius and radius of curvature at the output of the system (ω^{out} and R^{out}) are given as:

$$\omega^{out} = \left[\frac{\lambda}{\pi \operatorname{Im} \left(-\frac{1}{q_{out}} \right)} \right], \quad (5)$$

$$R^{out} = \left[\operatorname{Re} \left(\frac{1}{q_{out}} \right) \right]^{-1} \quad (6)$$

while the beam waist of the output beam (ω_0^{out}) and the distance from the beam waist where (6) and (7) are obtained (z^{out}) can be calculated as:

$$\omega_0^{out} = \frac{\omega^{out}}{\left[1 + \left(\frac{\pi (\omega^{out})^2}{\lambda R^{out}} \right)^2 \right]^{0.5}}, \quad (7)$$

$$z^{out} = \frac{R^{out}}{1 + \left(\frac{\lambda R^{out}}{\pi (\omega^{out})^2} \right)^2}. \quad (8)$$

Then, the transverse field distribution of the fundamental mode at z^{out} is obtained [11]:

$$E(r, z^{out}) = \left[\frac{2}{\pi \cdot (\omega^{out})^2} \right]^{0.5} \cdot \exp \left[-\frac{r^2}{(\omega^{out})^2} - j \frac{2 \cdot \pi}{\lambda} z^{out} - j \frac{\pi r^2}{\lambda R^{out}} + j \phi_0(z^{out}) \right] \quad (9)$$

$$\phi_0(z^{out}) = \tan^{-1} \left(\frac{\lambda \cdot z^{out}}{\pi \cdot \omega_0^2} \right) \quad (10)$$

where r represents the perpendicular distance from the axis of propagation and $\phi_0(z^{out})$ is the phase shift from the beam waist. Now it is easy to obtain the -3 dB beamwidth of (10) and, as a consequence, the spot size.

In Fig. 3 (a), the size of the semi-spot (half the beam) at a distance of 5 m as a function of f_1 and f_2 when $d_1 = 306.7$ mm (300 mm distance between horn aperture and first thin lens + 6.7 mm distance from beam waist to horn aperture) and $d_2 = 500$ mm is depicted. Semi-spots larger than 15 mm have been fixed to 15 mm in order to have a friendlier picture. From Fig. 3 (a) it can be seen that for the shown values for f_1 and f_2 , only a very small margin of values (associated to the central strip) satisfy the resolution goal. A pair of f_1 and f_2 having 5 mm semi-spot is highlighted. A similar plot can be obtained for different

distances d_1 and d_2 , as well as for different target distances (d_3). The overall simulation time on an Intel(R) Core(TM) i5 CPU at 2.67 GHz has been 2 minutes.

The idea after the QO design is to convert QO parameters into physical ones. Each thin lens is converted into an elliptical mirror and it has been observed that the mirror that imposes the dimension of the overall system is the second one (second thin lens, f_2) since it is the biggest. For that reason, a study on the second mirror diameter depending on the other parameters has been undertaken. QO Gaussian beam propagation theory states that a diameter of four times the beam radius (4ω) truncates the beam at a level 34.7 dB below that on the axis of propagation and includes 99.97% of the power in the fundamental mode Gaussian beam. This is generally sufficient to make the effects of diffraction by the truncation quite small. So the minimum diameter of that mirror has been obtained by taking into account that it must be at least four times the beam radius [11].

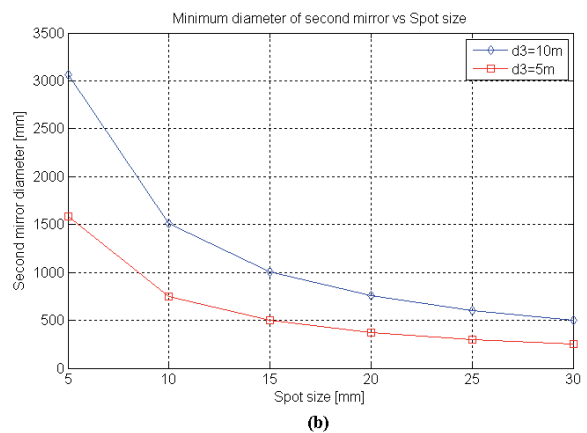
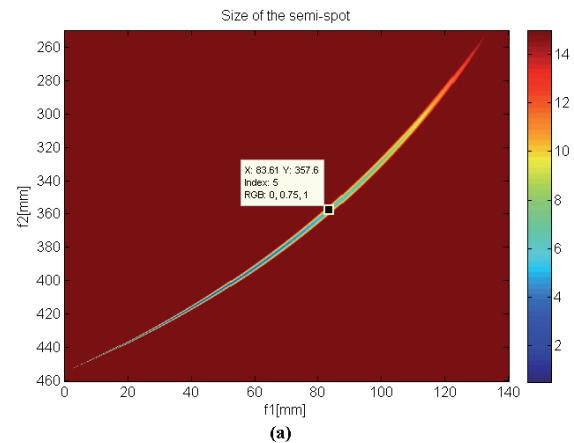


Fig. 3. (a) Size of the semi-spot as a function of the focus of the two thin lenses with $d_1 = 306.7$ mm and $d_2 = 500$ mm. (b) Second elliptical mirror diameter as a function of the desired spot size and target distance.

It has been observed that the smallest diameter of the second mirror that can be obtained does not depend on the distances d_1 and d_2 nor on f_1 and f_2 , and it is imposed by the target distance d_3 and by the spot size. Fig. 3 (b) shows the minimum diameter of the second mirror as a function of the

desired spot size for two different target distances (5 m and 10 m).

d_1 [mm]	d_2 [mm]	d_3 [mm]	f_1 [mm]	f_2 [mm]
306.7	500	5000	83.86	357.15

Tab. 1. QO parameters.

Once the minimum diameter has been obtained, the pair f_1 and f_2 which obtains that value for the pair $d_1 = 306.7$ mm and $d_2 = 500$ mm is selected and the focusing system based on thin lenses is designed. The main parameters of the system are presented in Tab. 1. With those parameters, $\omega^{out} = 8.31$ mm, $R^{out} = 3973$ mm, $\omega_0^{out} = 8.30$ mm and $z_{out} = 11.81$ mm are obtained, with a diameter spot size of 10 mm at 5 m target distance. It can be noted that the beam waist is not exactly at 5000 mm (target distance) but very close ($d_3 + z_{out} = 5011.81$ mm).

3. System Validation

The previously designed focusing system using QO theory has been validated by using the commercial electromagnetic simulation software, GRASP [12], in order to validate the design process. The methods used by GRASP are the highly efficient PO (Physical Optics) algorithms and the GTD (General Theory of Diffraction). The first step consists on translating the QO parameters obtained in the previous section when we use thin lenses into physical parameters to build the elliptical mirrors. This relationship is given by:

$$f = \frac{R_1 \cdot R_2}{R_1 + R_2} \tag{11}$$

where R_1 is the distance from the elliptical mirror to its input focus and R_2 is the distance from the elliptical mirror to its output focus. Following the labels in Fig. 4 (a), R_1 will be equal to the distance from the waist of the horn antenna to the first elliptical mirror; R_2 will be the distance from the first elliptical mirror to the common focus; R_3 will be the distance from that common focus to the second elliptical mirror; and R_4 will be the distance from the second mirror to the output focus. For the particular case represented in Tab. 1:

$$\left. \begin{aligned} R_1 &= d_1 = 306.7 \text{ mm} \\ f_1 &= 83.86 \text{ mm} \end{aligned} \right\} \rightarrow R_2 = \frac{R_1 \cdot f_1}{R_1 - f_1} = 115.42 \text{ mm} \tag{12}$$

$$\left. \begin{aligned} R_3 &= d_2 - R_2 = 384.58 \text{ mm} \\ f_2 &= 357.15 \text{ mm} \end{aligned} \right\} \rightarrow R_4 = \frac{R_3 \cdot f_2}{R_3 - f_2} = 5007.1 \text{ mm} \tag{13}$$

The obtained parameters for the system are summarized in Tab. 2. The angles have been chosen to reduce the overall size of it.

R_1 [mm]	R_2 [mm]	R_3 [mm]	R_4 [mm]	$2\alpha_1$ [°]	$2\alpha_2$ [°]
306.7	115.4	384.6	5007.1	60	60

Tab. 2. Physical parameters of elliptical mirrors.

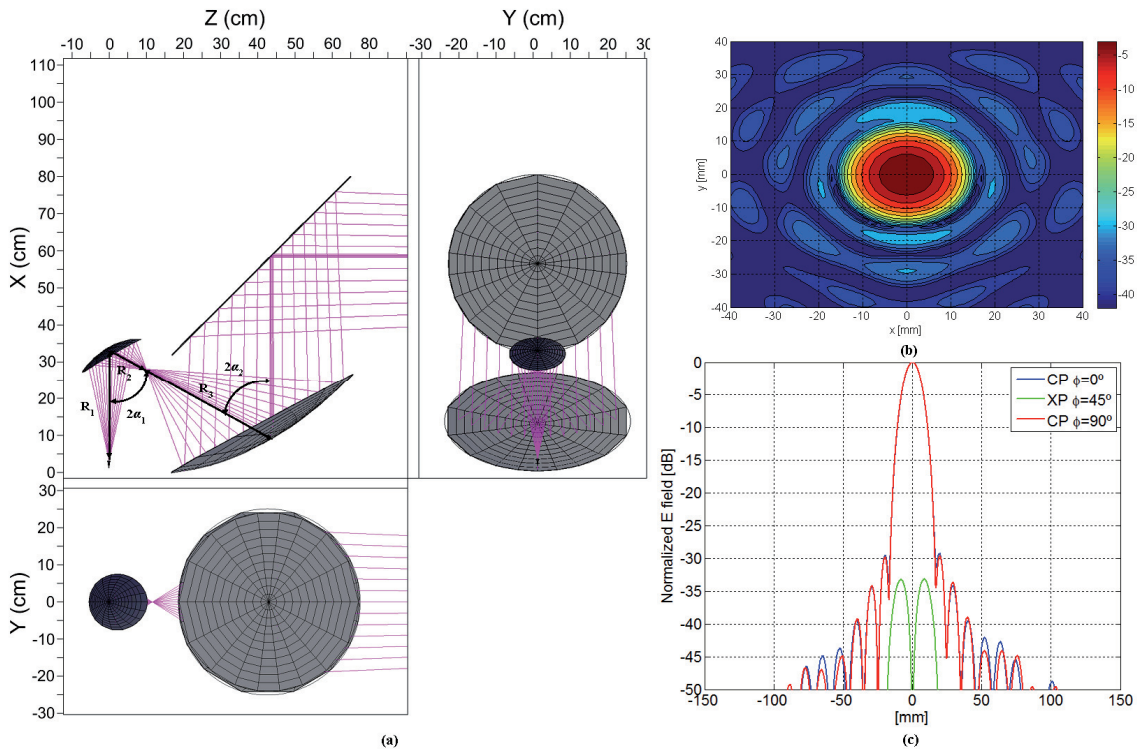


Fig. 4. (a) Designed focusing system to detect targets at 5 m with a resolution of 10 mm. Origin of coordinates is at the feed of the horn antenna. (b) 2D normalized E-field module at 5 m and (c) Co-polar and cross-polar component of the focusing system in three planes when no scanning is performed. Represented normalized E-field is calculated at detection distance (5 m).

The system with its physical dimensions can be seen in Fig. 4 (a). A plane mirror with a slightly larger diameter than the second elliptical mirror has been included in order to have a focusing system with scanning capabilities. This plane mirror is the only part of the system that is rotated to provide scanning capabilities. Diameters of the mirrors are 17 cm and 55 cm for elliptical ones and 68 cm for the plane one. The f/D ratios of the elliptical mirrors are 0.52 and 0.65 respectively. These values are in the range of $f/D \geq 0.5$ for $\alpha_i \leq 30^\circ$ which guarantee that the beam is almost not distorted [11], [13], [15].

The obtained spot with the focusing system at 5 m is plotted in Fig. 4 (b) and the radiation pattern at that distance in three different planes can be seen in Fig. 4 (c). It can be noted that the -3dB beamwidth is 10 mm, the side lobes are 30 dB lower than the main lobe in both $\varphi = 0^\circ$ (XZ plane) and $\varphi = 90^\circ$ (YZ plane) planes (with φ the angle defined over XY plane starting from x-axis) and the cross polar component is more than 30 dB lower in the $\varphi = 45^\circ$ plane. With this system 70.1 dBi gain is obtained at 5 m and the overall simulation time on the same computer as in Section 2 was 1 hour and 51 minutes. From this simulation time it is clear that the optimization of the system takes a lot of time.

The scanning capabilities of the system have also been explored. As previously mentioned, a plane mirror at the output of the second elliptical mirror has been included to add scanning capabilities to the focusing system. Fig. 5(a) shows the $\varphi = 90^\circ$ cut at 5 m when the system is scanning in the $\varphi = 0^\circ$ plane. The same performance is obtained when the scanning is performed on the $\varphi = 90^\circ$ plane. The scale of the figure has been changed in order to appreciate the distortion of the beam in a better way. The radiation pattern is almost not distorted even when the displacement is relatively high (500 mm). A scanning displacement of 500 mm is equal to a rotation in the azimuth and elevation plane of the plane mirror of 2.85° respectively. The scanning can be realized by rotating the mirror about two perpendicular axes. It can be placed on an axis spinning with a typical rotation mirror of 600 RPM which causes a circular path at the target distance. A slower rotary stage turns the spinning axis in a direction perpendicular to it with a speed of about $1^\circ/\text{sec}$. This leads to linear movement of the circular path. With such set-up, the scanning of a 500 mm x 500 mm target placed at 5 m can be done in less than 10 s.

In addition, the distortion of the beam when the target is closer to or away from has also been analyzed. The results can be seen in Fig. 5(b). Positive displacements mean that the target is further away from the source while negative ones mean that the target is closer to the source. As we move away from the target distance the beam is distorted due to the fact that the beam is not in the output focus of the second elliptical mirror. Diffraction effects appear and, in some cases, even the beam losses its gaussianity. It can be noticed that the system is robust for displacements of a target distance up to half a meter closer to or away from.

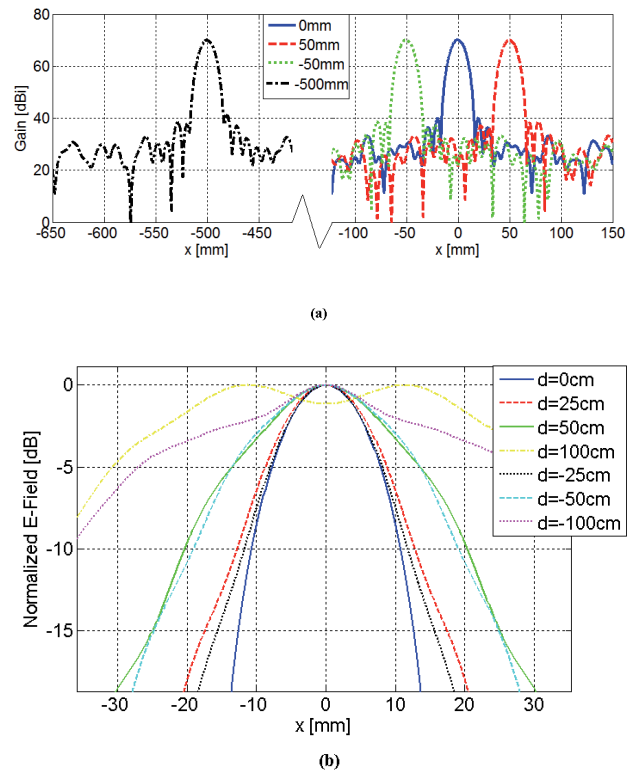


Fig. 5. (a) Scanning capability in the $\varphi = 0^\circ$ plane of the focusing system. (b) Normalized E-field vs the position for several displacement of the target distance. Represented normalized E-field is calculated at detection distance (5 m).

A very important issue that has to be taken into account when manufacturing the proposed system is the possible flaws associated to it. The most critical problems that may appear are changes in the roughness of the mirrors, as well as non-idealities on their borders. Since the mirrors have been designed in such a way that the beam is truncated at a power level of 34.7 dB below that on the axis of propagation, the effects of these last non-idealities can be neglected. As a consequence, the most important issue to be taken into account is the roughness of the surface of the mirrors. To do so, a parametric study has been carried out to check the system robustness against potential flaws in the manufacturing process. The surface roughness has been modeled as a zero mean uniform distribution with a variance of $20 \mu\text{m}$ that is 2% of the wavelength. This is a typical value for manufacturing tolerances of such mirrors. The obtained results (Fig. 6) are pretty similar to the ideal ones, and the only difference is that the secondary lobes level is higher than that of ideal mirrors. In any case, that level is 35 dB lower than the main lobe for places 50 mm far away from it. Then, the system is expected to be robust in terms of manufacturing flaws.

Once the spot, the scanning capabilities and the target distance displacements of the system have been analyzed, as well as manufacturing flaws, a simple software simulation of the behavior of the focusing system on a real environment has been undertaken. A target placed at 5 m (Fig. 7 (a)) has been scanned with the proposed system.

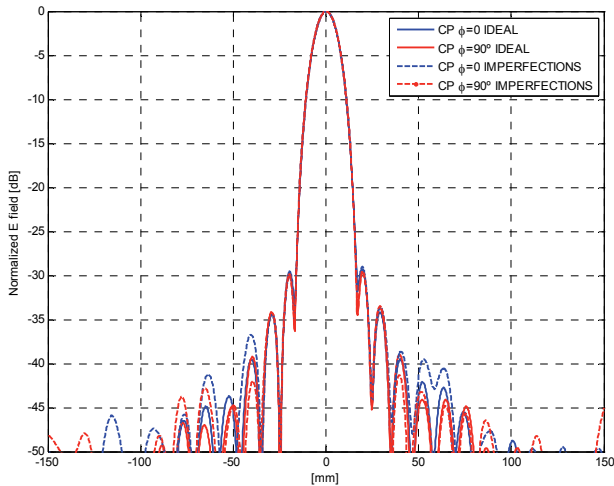


Fig. 6. Simulation of manufacture process imperfections. Continuous lines ($\phi = 0$ in blue and $\phi = 90^\circ$ in red cuts) represent the radiation pattern when perfect mirrors are used while dashed lines ($\phi = 0$ in blue and $\phi = 90^\circ$ in red cuts) represent the radiation pattern when a random distortion is inserted in the mirrors' surface. Represented normalized E-field is calculated at detection distance (5 m).

The size of two of the spots is plotted in the same scale as the scanning target in order to compare the size of them with the overall target (Fig. 7(b)). Four different hidden objects (a gun, a circle, a key and a cross) have been drawn inside the body of the target (Fig. 7 (c)) and the results obtained after scanning the target with the designed focusing system are plotted (Fig. 7(d)). The simulation consists on taking a picture of the target and turns it into a grey scale. After that, the metallic parts have been painted in white while the non-metallic parts have been painted in black. Then, the normalized spot at 5 m plotted in Fig. 4(b) is multiplied by that figure with displacements of 5 mm from left to right and up and down until the whole figure is scanned. It has to be mentioned that the simulation takes no

account of scattering properties, the return path loss and clothing effects, but it gives a general idea of how this focusing system will behave on an ideal environment. In the literature more sophisticated algorithms for radar target identification can be found [19].

4. Conclusion

A focusing system with a target distance of 5 m and a spot of 10 mm diameter spot size working at 300 GHz has been presented. The focusing system always work in the output focus of the second elliptical mirror, which means that the beam is almost not distorted when scanning. In addition, only the plane mirror rotates to provide scanning capabilities thus reducing the complexity of previous solutions. This focusing system needs to be included with all the necessary electrical components to generate the 300 GHz signal and with the signal processing capabilities to detect weapons or other objects hidden in the scanning targets to construct a terahertz radar.

The focusing system is based on a Gaussian telescope scheme and an analysis tool has been implemented in Matlab based on QO Gaussian beam propagation theory. With this tool, the basic parameters of them can be easily calculated to have the desired spot size and target distance.

Once the system based on thin lenses was designed, it has been transferred into elliptical mirrors with real dimensions and validated using a full-wave electromagnetic simulator. The obtained results agree with those previously reported by QO theory. With the proposed designing method, a robust focusing system with the desired resolution and target distance can be easily designed. The main advantages are that it reduces the computational resources needed and, as a consequence, the overall time for designing such kind of systems.

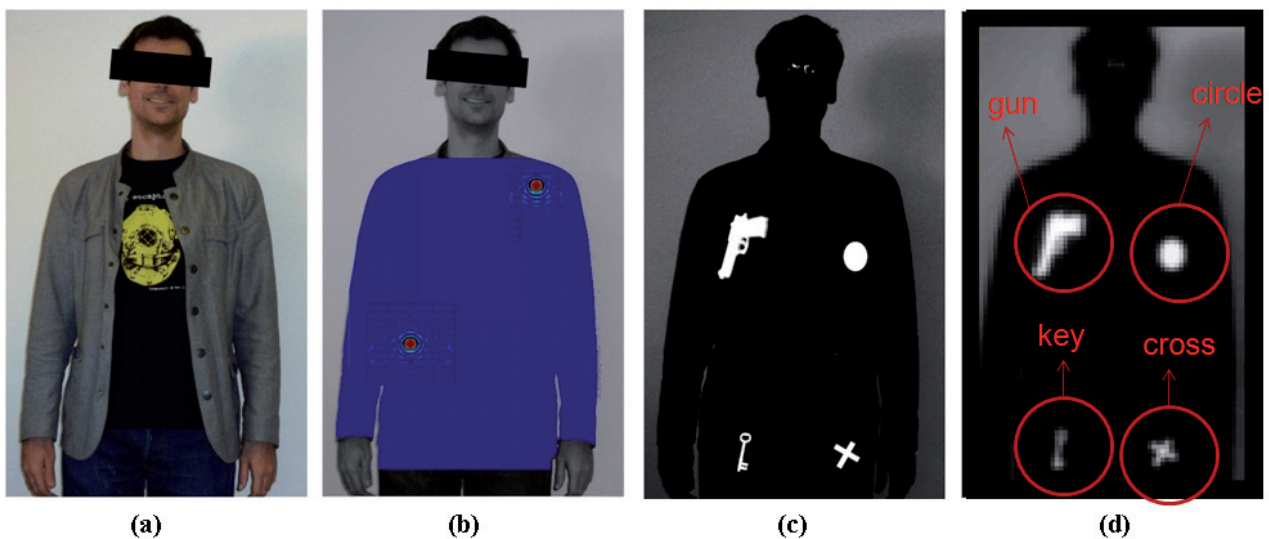


Fig. 7. Software simulation of the behavior of the first focusing system. (a) Photograph of the target we want to scan. (b) 2D normalized E-field module at 5 m together with the target to compare target and spot sizes. (c) Body of the target has been painted completely in black, while hidden items (key, gun, circle and cross) were painted in white. (d) Result of the simulation of scanning the picture in Fig. 7 (c) with the designed focusing system.

Moreover, scanning capabilities of the focusing system have been analyzed, showing great results because the beam is almost not distorted for large displacements of it along horizontal or vertical axis. Besides, the target can be half a meter closer to or away from the designed target distance (5 m) and the beam is almost not distorted. The flaws that may appear in the manufacturing process have been studied and the roughness of the surface of the mirrors has been simulated, concluding that the system is also robust against small changes in the surface of the mirrors. The absence of distortion on the beam, as well as its simplicity, makes the proposed focusing system suitable for target detection applications at THz and sub-THz frequencies.

Acknowledgements

This work was partially granted by CONSOLIDER-INGENIO 2010 CSD2008-00068 and CICYT Neolmag TEC2009-14525-C01. Work of Javier Montero-de-Paz was supported by the Spanish Education Minister under the program FPU (AP2009-4679). The authors want to thank Fundación Cajamadrid for his help during this work. The authors would like to thank Dr. O. Garcia-Perez, A. Rivera-Lavado, E. Ugarte-Muñoz and M. Molina-Romero from Carlos III University, and Dr. T. Finn and Dr. J. A. López from the Astronomy Observatory of Yebes (CAY) for their technical support in the validation of the system.

References

- [1] SIEGEL, P. H. Terahertz technology. *IEEE Trans. on Microwave Theory and Tech.*, March 2002, vol. 50, no. 3, p. 910 - 928.
- [2] CAI, M., LI, E. P. A novel terahertz sensing device comprising of a parabolic reflective surface and a bi-conical structure. *Progress in Electromagnetics Research*, 2009, vol. 97, p. 61-73.
- [3] JANSEN, C., WIETZKE, S., PETERS, O., SCHELLER, M., VIEWEG, N., SALHI, M., KRUMBHOLZ, N., JÖRDENS, C., HOCHREIN, T., KOCH, M. Terahertz imaging: applications and perspectives. *Applied Optics*, May 2010, vol. 49, no. 19, p. E48-E57.
- [4] LIZARRAGA, J., DEL-RIO, C. Resolution capabilities of future THz cameras. *Radioengineering*, June 2011, vol. 20, no. 2, p. 373 to 379.
- [5] KAPILEVICH, B., PINHASI, Y., ARUSI, R., ANISIMOV, M., HARDON, D., LITVAK, B., WOOL, Y. 330 GHz FMCW Image sensor for homeland security applications. *Journal of Infrared, Millimeter and Terahertz Waves*, September 2010, vol. 31, no. 11, p. 1370-1381.
- [6] DEMIRCI, S., CETINKAYA, H., YIGIT, E., OZDEMIR, C., VERTIY, A. A study on millimeter-wave imaging of concealed objects: Application using back-projection algorithm. *Progress in Electromagnetics Research*, 2012, vol. 128, p. 457-477.
- [7] COOPER, K. B., DENGLER, R. J., LOMBART, N., BRYLLERT, T., CHATTOPADHYAY, G., SCHLECHT, E., GILL, J., LEE, C., SKALARE, A., MEHDI, I., SIEGEL, P. H., Penetrating 3-D imaging at 4- and 25-m range using a submillimeter-wave radar. *IEEE Transactions on Microwave Theory and Techniques*, December 2008, vol. 56, no. 12.
- [8] EDERRA, I., GONZALO, R., ALDERMAN, B. E. J., HUGGARD, P. G., DE HON, B. P., VAN BEURDEN, M. C., MURK, A., MARCHAND, L., DE MAAGT, P. Sub-millimeter wave imaging array at 500 GHz based on 3-D electromagnetic band-gap material. *IEEE Transactions on Microwave Theory and Techniques*, November 2008, vol. 56, no. 11, p. 2256-2265.
- [9] HARMER, S. W., COLE, S. E., BOWRING, N. J., REZGUI, N. D., ANDREWS, D. On body concealed weapon detection using a phased antenna array. *Progress in Electromagnetics Research*, 2012, vol. 124, p. 187-210.
- [10] ANDRES-GARCIA, B., GARCIA-MUÑOZ, L. E., SEGOVIA-VARGAS, D. Ultrawideband antenna excited by a photomixer for terahertz band. *Progress in Electromagnetics Research*, February 2011, vol. 114, p. 1-15.
- [11] GOLDSMITH, P. F. *Quasioptical Systems: Gaussian Beam Quasioptical Propagation and Applications*. New York: IEEE Press/Chapman and Hall, 1998.
- [12] GRASP, *General Reflector and Antenna arm analysis software*, <http://www.ticra.com/what-we-do/software-descriptions/grasp/>, June 2012.
- [13] MURPHY, J. A. Distortion of a simple Gaussian beam on reflection from off-axis ellipsoidal mirrors. *International Journal of Infrared and Millimeter Waves*, September 1987, vol. 8, no. 9, p. 1165-1186.
- [14] BARYSHEV, A., WILD, W. ALMA band 9 optical layout. ALMA Memo #394, 2001.
- [15] MURPHY, J. A., WITHINGTON, S. Perturbation analysis of Gaussian-beam-mode scattering at off-axis ellipsoidal mirrors. *Infrared Physics and Technology*, 1996, vol. 37, p. 205-219.
- [16] WYLDE, R. J. Millimeter-wave Gaussian beam-mode optics and corrugated feed horns. *IEE Proceedings*, August 1984, vol. 131, no. 4.
- [17] MOLINA-ROMERO, M. Implementación de una herramienta para el estudio rápido de sistemas cuasi-ópticos. Master Thesis Dissertation, Universidad Carlos III de Madrid, Leganés, 2010 (in Spanish).
- [18] MATLAB, <http://www.mathworks.com/>, June 2012.
- [19] KABOUREK, V., ČERNÝ, P., MAZÁNEK, M. Clutter reduction based on principal component analysis technique for hidden objects detection. *Radioengineering*, April 2012, vol. 21, no. 1, p. 464 - 470.

About Authors ...

Javier MONTERO-DE-PAZ was born in Madrid, Spain, on May 29, 1984. He received the M.Sc. in Telecommunications from Carlos III University, Madrid, Spain, in 2009, and is currently working toward the Ph.D. degree in Communications at Carlos III University. His research lines are metamaterials, active antennas, Schottky diodes, dielectric lenses and terahertz antennas.

Luis Enrique GARCIA-MUÑOZ is an Associate Professor at the Universidad Carlos III de Madrid, Spain. He has managed or participated in several national and European research projects on areas such as antennas and array design. He has coauthored more than 50 papers in international journals and conferences and holds three patents. His current research interests include terahertz antennas, array design, truncation in antenna arrays and radioastronomy instrumentation.

Daniel SEGOVIA-VARGAS was born in Madrid, Spain, in 1968. He received the Telecommunication Engineering degree and the Ph.D. degree from the Polytechnic University of Madrid, in 1993 and in 1998, respectively. From 1993 to 1998, he was an Assistant Professor at Valladolid University. Since 1999, he is an Associate Professor at Carlos III University in Madrid where he is in charge of the Microwaves and Antenna courses. Since 2004, he is the

Leader of the Radiofrequency Group, Dept. of Signal Theory and Communications, University Carlos III of Madrid. He has authored and coauthored over 110 technical conference, letters and journal papers. His research areas are printed antennas and active radiators and arrays, broadband antennas, LH metamaterials, terahertz antennas and passive circuits. He has also been expert of the European Projects Cost260, Cost284 and COST IC0603.